Scientific Research Publishing

World Journal of Condensed Matter Physics, 2018, 8, 171-184
http://www.scirp.org/journal/wjcmp
ISSN Online: 2160-6927
ISSN Print: 2160-6919

Interaction in the Steady State between Electromagnetic Waves and Matter

Aidan L. Gordon, Giovanna Scarel*

Department of Physics and Astronomy, James Madison University, Harrisonburg, VA, USA
Email: *scarelgx@jmu.edu

How to cite this paper: Gordon, A.L. and Scarel, G. (2018) Interaction in the Steady State between Electromagnetic Waves and Matter. *World Journal of Condensed Matter Physics*, **8**, 171-184.
https://doi.org/10.4236/wjcmp.2018.84012

Received: October 19, 2018
Accepted: November 9, 2018
Published: November 12, 2018

Abstract

It is common experience that our eyes do not perceive significant changes in color when we observe for long time an object continuously exposed to light. We always see plants to be green in summer until in autumn factors external to our vision, such as changes in the length of daylight and temperature, cause the break-down of chlorophyll and, in turn, spectacular changes in plant's colors. Likewise, the photocurrent produced in solar panels or field effect transistors achieves a steady state magnitude shortly after the start of the illumination. The steady state photocurrent lasts until the illumination stops. Understanding the origin of the steady state response of a device or light harvesting (LH) system to illumination with electromagnetic (EM) waves motivates the research presented in this work. In our experiments, we used capacitors as LH systems and illuminated them with infrared (IR) light over an 80 hours time period. We investigated the interaction between light and matter by monitoring versus time the voltage output of the capacitors. By combining modeling and experimental observations, we concluded that the steady state voltage is established soon after the start of the illumination as the consequence of the law of conservation of energy. We also found that the magnitude of the voltage in the steady state depends on the power and period of the illuminating IR light, and on the capacitance of the capacitor. When light's power undergoes fluctuations, also the voltage produced by the capacitor and the surface charge density on the capacitors do so. These findings suggest that the law of conservation of energy has a significant repercussion when light is absorbed by matter in the steady state, for example in the mechanism of vision in vertebrates. Likewise, these findings are true when light is emitted from matter, for example in the mechanism of formation of the Cosmic Microwave Background (CMB).

Keywords

Infrared, Light-Matter Interaction, Conservation of Energy, Steady State

1. Introduction

Is exposure time important in light-matter interaction? The question arises naturally when considering light as a wave. In this case, the energy transferred to matter is $P\Delta t$, where Δt is a time interval [1]. The average power $P \propto |\boldsymbol{E}|^2$, where $\boldsymbol{E}$ is the wave's electric field, can easily be measured with a power sensor. Therefore, because of the dependence on Δt of the transferred energy, when matter is exposed to light, two scenarios might occur: in the first scenario, the energy transferred from light to matter increases with time. In the second scenario, the energy transferred from light to matter reaches a steady state. By exploring the first scenario, we unveil outstanding consequences. One is that a prolonged and continuous exposure of a field effect transistor (FET) to light would increase with time the magnitude of the produced photocurrent. Another consequence is that the passing of time would change all year long the color of plants exposed to light, not just in autumn when chlorophyll breaks down due to the shortening of daylight and to temperature decrease. An additional consequence is that prolonged exposure to solar light of the photoreceptor cells (rods, cones and photosentitive retinal ganglion cells) in vertebrate's eyes would increase the magnitude of the action potential V_{ap} produced in the process enabling vision. This increase would be such that $P\Delta t \propto V_{ap}^2$ [1]. A further consequence would be the increase with exposure time Δt of a rotation rate ρ_{rot} such that $P\Delta t \approx \frac{1}{2} I_{exp} \rho_{rot}^2$, where I_{exp} is a moment of inertia. Such a situation could occur to a support plate in a microwave oven irradiated by microwaves [1]. As a final consequence, we mention that the frequency ν_{CMB} of the cosmic microwave background (CMB) radiation would increase with time after its initial emission since $\Delta t \propto \nu_{\mathrm{CMB}}^2$, as we will discuss elsewhere.

Considering experimental results, however, leads to conclusions different than those just described. For example, Sarker *et al.* [2] suggest that photocurrent production in FETs reaches a steady state rather than indefinitely increasing with time. Our own experience indicates that no significant changes in color occur in plants in the three-month summer period, until in autumn the significant and steady variations in temperature and daylight change this trend. In general, from our own experience of vision, we know that colors remain steady unless something happens in the environment. Thus, we must admit that a drift in the magnitude of the action potential V_{ap} with time of exposure to light of the photoreceptor cells does not occur. We can explain this fact either by assuming that V_{ap} reaches a steady state upon hyperpolarization of the photoreceptor cells, or via other phenomena, such as thermal energy dissipation or mechanical motion, arising to keep V_{ap} constant. We will show elsewhere that the steady state value of the action potential V_{ap} upon hyperpolarization is the result of the evolutionary adaptation of the vertebrate's vision to the average power of solar light (136 mW/cm^2 [3] [4]). Moreover, everyday experience shows us that the rotation rate ρ_{rot} of the support plate in a microwave is not accelerated by a prolonged exposure to the microwaves. Finally, accurate measurements of the frequency of

the CMB radiation convey that it peaks at $\nu_{\text{CMB}} = 160.23$ GHz, which makes the CMB radiation uniquely identifiable [5]. These experimental evidences strongly suggest that with time the energy transferred from light to matter reaches a steady state in agreement with the second scenario.

In this work, we embrace the second scenario and show that achieving a steady state illumination (ssi) follows from the description of light-matter interaction through the law of conservation of energy. To achieve this conclusion, we study experimentally and through modeling the magnitude of the voltage $V(t)$ and temperature difference $\Delta T(t)$ versus time produced by the interaction of infrared (IR) light with a capacitor. We observe that, upon illuminating with IR light the capacitor for hours or days, the voltage $V(t)$ levels off in the ssi regime at a value $V_{ssi} = \lim_{t\to\infty} V(t)$. We assume that in the ssi the voltage $V(t)$ produced by the capacitor, the temperature difference $\Delta T(t)$ and the surface charge $q(t)$ are constant. However, fluctuations can occur in the average power $P(t)$ of the IR light due to the operation of the Q301 globar source as described in Ref. [6]. These fluctuations trigger perturbations of $V(t)$, $\Delta T(t)$ and $q(t)$. The perturbations in $V(t)$ and $\Delta T(t)$ can experimentally be observed [1] [6] [7], but those in $q(t)$ and in the surface charge density $\sigma(t)$ cannot be detected. Nevertheless, literature results support evidences for the existence of such perturbations. For instance, light with wavelength from 1600 nm to 700 nm was found to trigger changes in the surface charge density $\sigma(t)$ in polyethylene [8] with magnitude dependent upon the IR light's power over area, *i.e.* the intensity, and with a charge responsivity of about 5.3 pC/W [8]. The fluctuations in the charge density were found not to be related to heating effects, in agreement with results of Ref. [1]. Thus, supported by experimental observations and by modeling, we incorporate into the energy conservation equation describing the interaction of IR light with matter [1] [6] the experimentally observed sinusoidal fluctuations of the average power $P(t)$ of the IR light, and, consequently, of the voltage $V(t)$ and temperature difference $\Delta T(t)$. Then, we derive the surface charge density $\sigma(t) = \dfrac{q(t)}{A_{cs}}$ versus time [1], where A_{cs} is the illuminated area with diameter D of the capacitor, from the best match between the voltage $V(t)$ derived from the energy conservation equation and the experimentally observed $V(t)$. This result extends to the ssi regime the validity of the law conservation of energy for the transfer of energy from light to matter. The role of this law was initially established in the exponential perturbation regime (EPR) immediately following the start of the illumination with IR light [1] [7]. The importance of these findings is that they help understanding several natural phenomena such as the generation of the CMB and the mechanism of vision in vertebrates that we will discuss elsewhere.

2. Experimental Set-Up

Capacitors: We studied the interaction of IR light with matter through the vol-

tage $V(t)$ produced in time t by a 07111-9L31-04B device manufactured by Custom Thermolectric Inc. The basic device, illustrated in **Figure 1**, is a thermoelectric device consisting of a sequence of layers: 1) an insulating alumina (AlO) plate on the face exposed to the IR light, 2) a metallic Cu plate, 3) a layer of pillars made of a doped semiconducting Bi_2Te_3-based alloy, 4) another Cu plate, and 5) another AlO plate. This multi-layer structure resembles that of a capacitor, as shown in previous research [1] [6] [7]. To change the capacitance C of the capacitor we combined the capacitors in series or added a layer of insulating tape (IT) on the face exposed to the IR light. The IT consists of heavy cotton cloth pressure sensitive tape with strong adhesive and tensile properties. In this research we used three specific structures: two capacitors in series with IT as in **Figure 1(a)** featuring $C = 148.5$ pF, one capacitor with IT as in **Figure 1(b)** with $C = 298.1$ pF, and two capacitors without IT as in **Figure 1(c)** enabling $C = 526.9$ pF.

Infrared light: We used the continuous broadband IR light in the 350 - 7500 cm^{-1} wavenumber (28,600 nm - 1300 nm wavelength or 95.33 fs - 4.33 fs period) range produced by a Q301 globar source in a N_2-purged Bruker Vertex 70 spectrometer [6] [7]. The beam diameter is $D = 10$ mm. The average power is $P = 25$ mW between 700 - 7500 cm^{-1} (14,286 nm - 1300 nm, or 47.62 fs - 4.33 fs period, the middle IR (MIR) range) and about 21.2 μW between 350 - 700 cm^{-1} (28,600 nm - 14,286 nm or 95.33 fs - 47.62 fs, the far IR (FIR) range). We placed a polyethylene polarizer (Pike Technologies) with a 500 - 10 cm^{-1} spectral range between the IR light and the capacitor to achieve the 21.2 μW average power in the FIR range. We monitored versus time t the average power $P(t)$ of the IR light in the MIR range using a power-meter sensor Coherent PowerMax RS PS19, sensitive to the 300 - 11,000 nm wavelength range and to the 100 μW to 1 W power range.

Temperature measurements: We measured the temperatures of the illuminated ($T_{light}(t)$) and non-illuminated ($T_{no\text{-}light}(t)$) faces of the capacitors using OMEGA type E Ni-Cr/Cu-Ni thermocouple probes [1] [6] [7].

Data collection: We exposed the capacitors to IR light for ~80 hours after starting the illumination, and collected the voltage $V(t)$, the temperature difference $\Delta T(t)$, the $T_{light}(t)$) and $T_{no\text{-}light}(t)$ temperatures versus time t for the entire duration of the measurements in the ssi. The data were collected using LabView 2012 and a National Instruments PXI-1042q communications chassis [1] [6] [7].

3. Results

To investigate the magnitude of the voltage versus time $V(t)$ in the ssi, we collected for ~80 hours the voltage $V(t)$ generated by a capacitor interacting with IR light. This amount of time assures that fluctuations can be observed. Without fluctuations of the average power $P(t)$ we expect the voltage in the ssi to be $V_{ssi} = V_0 + \Delta V$, where V_0 is the voltage before the start of the illumination with IR light and ΔV the jump in voltage in the EPR with a time constant

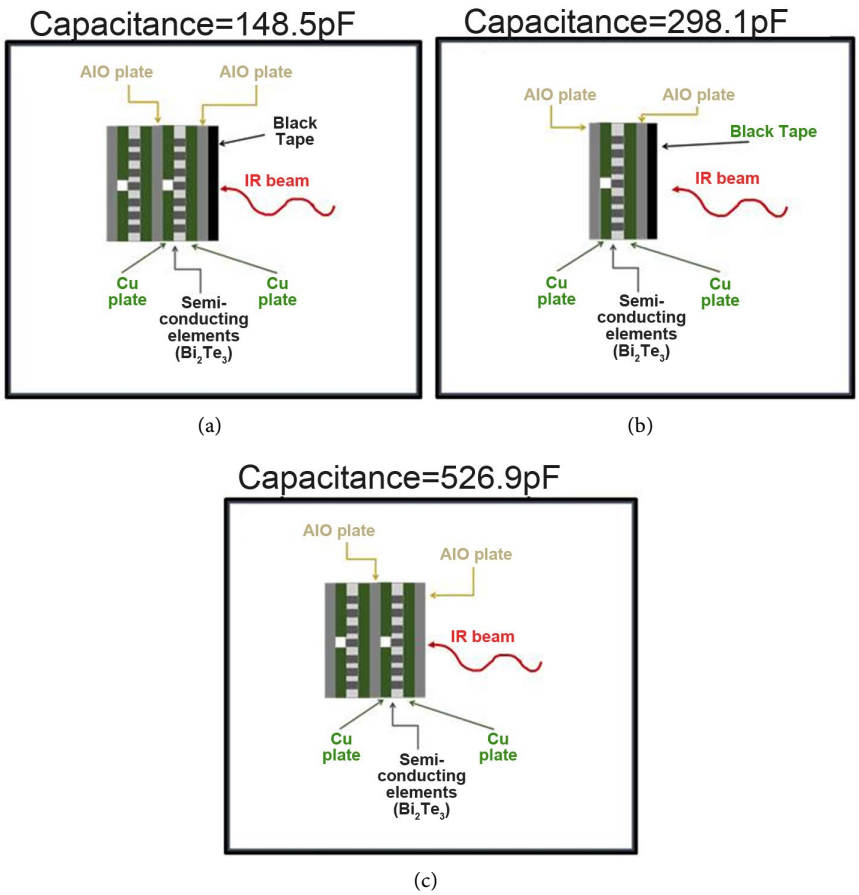

Figure 1. The cross-section of the capacitors used in this research consists of a layer of Bi_2Te_3 semiconducting elements embedded between alumina (AlO) and Cu plates. Configuration (a) illustrates two capacitors in series with insulating tape (IT) on the illuminated face. This combination features a capacitance $C = 148.5$ pF. Configuration (b) depicts one capacitor with IT on the face exposed to the IR light which enables $C = 298.1$ pF. Configuration (c) pictures two capacitors in series without IT on the face exposed to the IR light allowing $C = 526.9$ pF. The IT consists of heavy cotton cloth pressure sensitive tape with strong adhesive and tensile properties.

of tens of seconds [1]. With sinusoidal fluctuations arising in $P(t)$, in time we expect perturbations to occur in the voltage $V(t)$, the temperature difference $\Delta T(t)$, the surface charge $q(t)$ and the surface charge density $\sigma(t)$ [1] [6] [8]. In particular, the experimentally observable $V(t)$ is such that $V(t) = V_{ssi} + F(t)$, where $F(t)$ is the perturbation transferred by the fluctuations to $V(t)$. This perturbation justifies the non-constant trends of the voltage $V(t)$ in the ssi, as we observe in **Figure 2**. Here, all the panels show that $V(t)$ achieves a minimum or various minima over a time interval several hours long. Specifically, **Figure 2(a)** shows the case of a capacitor with $C = 148.5$ pF placed at an angle $\theta_0 = 0^\circ$ with respect to the illuminating IR light with period $\tau \cong 83$ fs and average power $P_{ssi} \cong 21.2\ \mu$W. In this case, $V_{ssi} = 0.25$ mV and the sinusoidal fluctuations of $P(t)$ generate a minimum voltage $V_{\min} = 0.20$ mV occurring in $V(t)$ 56 hours after the start of the illumination. **Figure 2(b)** illustrates the case of

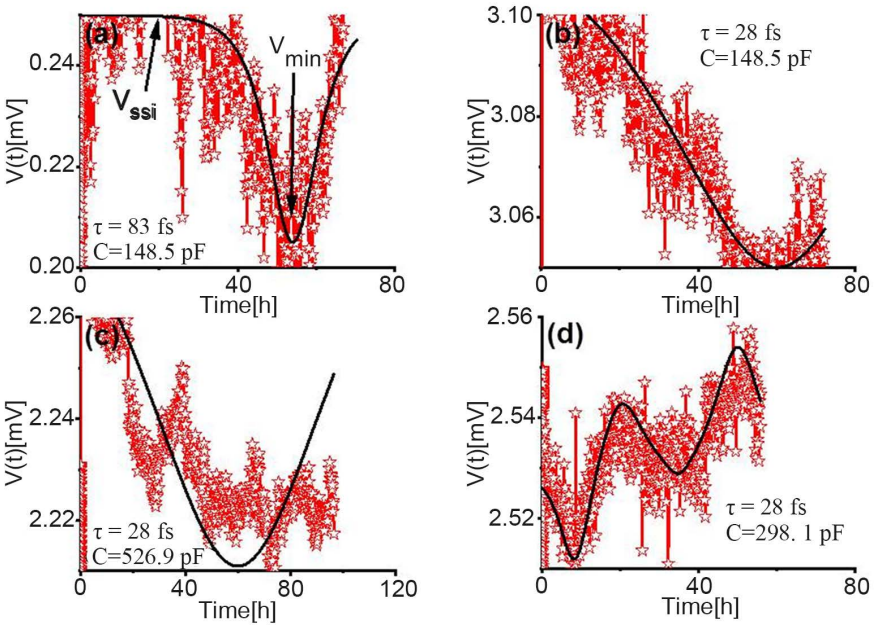

Figure 2. The variation of voltage versus time $V(t)$ in the time interval of ~80 hours after starting the illumination with IR light. The experimental data are presented along with the fitting line (continuous black line) derived from Equation (1). We selected four cases with different angle of incidence θ_0, capacitance C, period τ, and average power P. (a) $\theta_0 = 0^\circ$, $C = 148.5$ pF, $\tau = 83$ fs, $P_{ssi} \cong 21.2$ μW, average voltage in the steady state illumination (ssi) $V_{ssi} = 0.25$ mV, and $V_{\min} = 0.20$ mV occurring 56 hours after the start of the illumination. The V_{ssi} and the $V_{\min}$ are labelled in the panel; (b) $\theta_0 = 0^\circ$, $C = 148.5$ pF, $\tau = 28$ fs, $P \cong 25$ mW, $V_{ssi} = 3.10$ mV, and $V_{\min} = 3.05$ mV occurring 60 hours after the start of the illumination; (c) $\theta_0 = 45^\circ$, $C = 526.9$ pF, $\tau = 28$ fs, $P \cong 25$ mW, $V_{ssi} = 2.27$ mV, and $V_{\min} = 2.22$ mV occurring 60 hours after the start of the illumination; (d) $\theta_0 = 45^\circ$, $C = 298.1$ pF, $\tau = 28$ fs, $P \cong 25$ mW, $V_{ssi} = 2.54$ mV, and $V_{\min} = 2.51$ mV occurring 8 hours after the start of the illumination.

a capacitor with $C = 148.5$ pF and $\theta_0 = 0^\circ$, illuminated with IR light at $\tau \cong 28$ fs and $P_{ssi} \cong 25$ mW. In this case, $V_{ssi} = 3.10$ mV, and a minimum at $V_{\min} = 3.05$ mV emerges in $V(t)$ 60 hours following the start of the illumination. **Figure 2(c)**, on the other hand, depicts the case for $C = 526.9$ pF, $\theta_0 = 45^\circ$, $\tau \cong 28$ fs and $P_{ssi} \cong 25$ mW. In this case, $V_{ssi} = 2.27$ mV, and a minimum at $V_{\min} = 2.22$ mV in $V(t)$ is produced 60 hours after the start of the illumination. Finally, **Figure 2(d)** pictures the case for $C = 298.1$ pF, $\theta_0 = 45^\circ$, $\tau \cong 28$ fs and $P_{ssi} \cong 25$ mW. In this case $V_{ssi} = 2.54$ mV, and various minima are generated in $V(t)$, the first of which with $V_{\min} = 2.51$ mV appears 8 hours after the start of the illumination.

In each panel of **Figure 2**, $V(t)$ can be fitted using a hyperbolic secant function [6]:

$$V(t) = V_{ssi} + V_{osc}\,\mathrm{sech}\left(\frac{t - t_{cV}}{H_V}\right), \tag{1}$$

where V_{osc} is the oscillation in the voltage due to the quasi-sinusoidal fluctuations of $P(t)$, t_{cV} is critical time of the voltage, and H_V is a time constant [6]. We will use the function in Equation (1) to validate with experimental data the model we developed for $V(t)$ based on the law of conservation of energy [1].

4. Model

To determine 1) the magnitude of V_{ssi}, 2) the surface charge density $\sigma(t)$, and 3) the mechanism that transfers to $V(t)$ the fluctuations of $P(t)$, we use the law of conservation of energy [1]:

$$E(t) = P(t)\tau = \frac{1}{2}CV(t)^2 + \frac{1}{2}\frac{q(t)^2}{C} - \Sigma_0 \Delta T(t), \tag{2}$$

where $E(t)$ is the energy transferred from the IR light to the capacitor, and Σ_0 is the entropy in a closed system derived as in Ref. [1].

1) Determining the magnitude of V_{ssi}

By manipulating Equation (2) we obtain the voltage $V(t)$ as:

$$V(t) = \sqrt{\frac{2}{C}P(t)\tau - \frac{q(t)^2}{C^2} + \frac{2\Sigma_0}{C}\Delta T(t)}. \tag{3}$$

In **Figure 3**, we display the voltage $V(t)$ modeled from Equation (3) alongside the fitting functions obtained with Equation (1) of the experimental voltage $V(t)$ of the four cases reported in **Figure 2**. The values of V_{ssi}, viewed as $V_{ssi} = \lim_{t\to\infty} V(t)$, are derived from the comparison between the panels in **Figure 3** and the plateau level achieved by the jump in voltage ΔV at the beginning of the illumination with IR light (the EPR) for the each of the capacitors under various illumination conditions. These jumps in voltage ΔV are pictured in **Figure 4**. Using the results from **Figure 3** and **Figure 4** we obtain the following values for V_{ssi} in the four examined cases: a) capacitance $C = 148.5$ pF and period $\tau = 83$ fs yield $V_{ssi} \cong 0.25$ mV, b) $C = 148.5$ pF and $\tau = 28$ fs produce $V_{ssi} \cong 3.10$ mV, c) $C = 526.9$ pF and $\tau = 28$ fs generate $V_{ssi} \cong 2.30$ mV, and finally d) $C = 298.1$ pF and $\tau = 28$ fs give rise to $V_{ssi} \cong 2.55$ mV. The good match between the values of V_{ssi} extracted from **Figure 3** and **Figure 4** suggests that the law of conservation of energy in Equation (2) describes in a satisfactory manner the light-matter interaction in the EPR and in the ssi. In both the EPR and the ssi, the unknown variables are Σ_0, $q(t)$ and $\sigma(t)$. The entropy Σ_0 can be derived as in Ref. [1] for the whole time interval that covers the EPR and the ssi. Whereas, the surface charge $q(t)$ and surface charge density $\sigma(t)$ in the ssi requires a more dedicated discussion which we present in the next Section.

2) Determining the surface charge density variation in time, $\sigma(t)$

To determine the surface charge $q(t)$ and the surface charge density $\sigma(t)$ in the ssi we proceed as in Ref. [1], which addressed the same issue in the EPR. In the ssi, as in the EPR, the average power $P(t)$ of the IR light acts on the

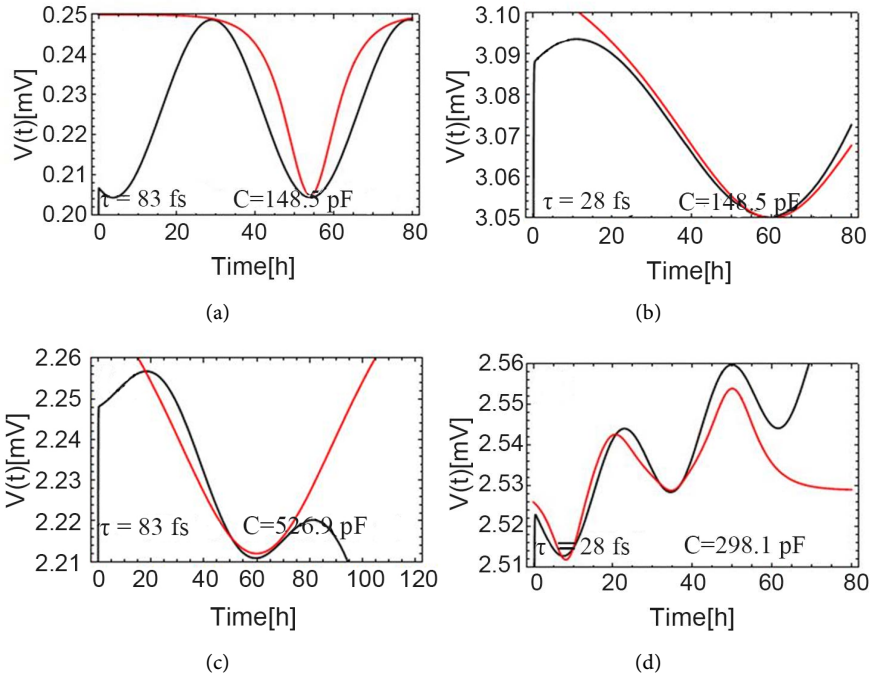

Figure 3. Experimental fitting line from Equation (1) (red line) and modeled line (black line) for different capacitors under various illumination conditions. The experimental fitting lines (red lines) correspond to those in **Figure 2**. The fluctuations in voltage occurring in the time interval of ~80 hours after starting the illumination with IR light are all of the same size, despite different capacitor and illumination conditions. We modeled the four cases reported in the panels using Equation (3) and the following parameters: (a) Angle of incidence $\theta_0 = 0^\circ$, capacitance $C = 148.5\ \text{pF}$, period $\tau = 83\ \text{fs}$, power in the steady state illumination (ssi) $P_{ssi} \cong 21.2\ \mu\text{W}$, oscillation in the power in the ssi $P_{osc} = 17.8\ \mu\text{W}$, entropy $\Sigma_0 = 0.58\times10^{-16}\ \text{J}/^\circ\text{C}$, temperature difference $\Delta T = 0.03^\circ\text{C}$, initial voltage in modeling $\Delta V_{0-\text{mod}} = -0.222\ \text{mV}$, surface charge density in the ssi $\sigma_{ssi} = 0.96\ \text{nC}/\text{m}^2$, oscillation in the surface charge density $\sigma_{osc} = 0.95\ \text{pC}/\text{m}^2$, critical time of the power $t_{cP} = 66.6\ \text{h}$ [5], and $H_p = 8\ \text{h}$ is $\frac{1}{4}$ of the period of the sinusoidal function describing the power (see Equation (4) and Ref. [6]); (b) $\theta_0 = 0^\circ$, $C = 148.5\ \text{pF}$, $\tau = 28\ \text{fs}$, $P_{ssi} = 25\ \text{mW}$, $P_{osc} = 0.25\ \text{mW}$, $\Sigma_0 = 25.9\times10^{-16}\ \text{J}/^\circ\text{C}$, $\Delta T = 0.27^\circ\text{C}$, $\Delta V_{0-\text{mod}} = 1.608\ \text{mV}$, $\sigma_{ssi} = 8.88\ \text{nC}/\text{m}^2$, $\sigma_{osc} = 0.00098\ \text{nC}/\text{m}^2$, $t_{cP} = 35\ \text{h}$, and $H_p = 19\ \text{h}$; (c) $\theta_0 = 45^\circ$, $C = 526.9\ \text{pF}$, $\tau = 28\ \text{fs}$, $P_{ssi} = 25\ \text{mW}$, $P_{osc} = 0.55\ \text{mW}$, $\Sigma_0 = 87.5\times10^{-16}\ \text{J}/^\circ\text{C}$, $\Delta T = 0.08^\circ\text{C}$, $\Delta V_{0-\text{mod}} = 0.33\ \text{mV}$, $\sigma_{ssi} = 25.58\ \text{nC}/\text{m}^2$, $\sigma_{osc} = 0.00098\ \text{nC}/\text{m}^2$, $t_{cP} = 39\ \text{h}$, and $H_p = 10\ \text{h}$; (d) $\theta_0 = 45^\circ$, $C = 298.1\ \text{pF}$, $\tau = 28\ \text{fs}$, $P_{ssi} = 25\ \text{mW}$, $P_{osc} = 0.25\ \text{mW}$, $\Sigma_0 = 63.6\times10^{-16}\ \text{J}/^\circ\text{C}$, $\Delta T = 0.11^\circ\text{C}$, $\Delta V_{0-\text{mod}} = 0.298\ \text{mV}$, $\sigma_{ssi} = 17.98\ \text{nC}/\text{m}^2$, $\sigma_{osc} = 0.00005\ \text{nC}/\text{m}^2$, $t_{cP} = 15.2\ \text{h}$, and $H_p = 4.3\ \text{h}$.

surface charges $q(t)$ on the capacitor with a force $\boldsymbol{f}(t) = q(t)\boldsymbol{E}(t)$. Such force displaces the charges away from the location in which the IR waves illuminate the capacitor, locally decreasing their surface density as $\sigma(\boldsymbol{r},t) \propto \frac{1}{P(t)}$. Due to the low power of the IR light, no charge is kicked out of the capacitor while a

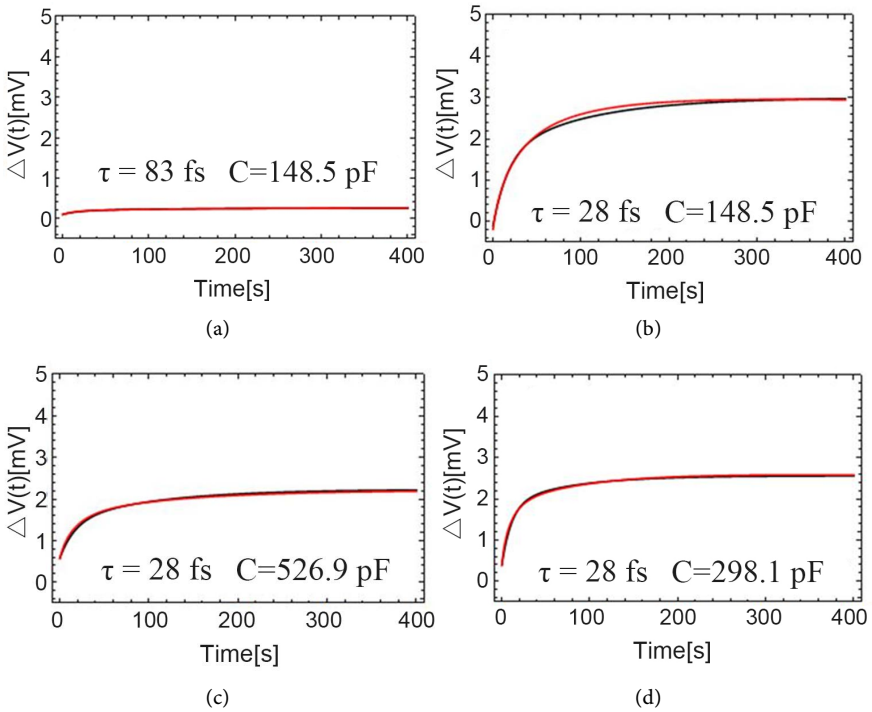

Figure 4. Experimental fitting line (red line) and modeled line (black line) for the jump in voltage ΔV occurring for different capacitors under various illumination conditions at the beginning of the illumination with IR light. It is noticeable that ΔV depends on capacitance C, period τ, and average power P. We performed the modeling for the cases reported in the panels using the following parameters: (a) Angle of incidence $\theta_0 = 0^\circ$, capacitance $C = 148.5$ pF, period $\tau = 83$ fs, power in the steady state illumination (ssi) $P_{ssi} \cong 21.2$ μW, oscillation in the power in the exponential perturbation regime (EPR) $P_{osc-EPR} = 21.2$ μW, entropy $\Sigma_0 = 0.58 \times 10^{-16}$ J/°C, temperature difference $\Delta T = 0.03$°C, initial voltage in modeling $\Delta V_{0-\mathrm{mod}} = 0.019$ mV, surface charge density in the ssi $\sigma_{ssi} = 0.96$ nC/m^2 and oscillation in the surface charge density $\sigma_{osc} = 0.95$ pC/m^2; (b) $\theta_0 = 0^\circ$, $C = 148.5$ pF, $\tau = 28$ fs, $P_{ssi} = 25$ mW, $P_{osc-EPR} = 25$ mW, $\Sigma_0 = 25.9 \times 10^{-16}$ J/°C, $\Delta T = 0.27$°C, $\Delta V_{0-\mathrm{mod}} = -1.06$ mV, $\sigma_{ssi} = 8.88$ nC/m^2 and $\sigma_{osc} = 0.098$ nC/m^2; (c) $\theta_0 = 45^\circ$, $C = 526.9$ pF, $\tau = 28$ fs, $P_{ssi} = 25$ mW, $P_{osc-EPR} = 25$ mW, $\Sigma_0 = 87.5 \times 10^{-16}$ J/°C, $\Delta T = 0.08$°C, $\Delta V_{0-\mathrm{mod}} = -0.1$ mV, $\sigma_{ssi} = 25.58$ nC/m^2 and $\sigma_{osc} = 0.00098$ nC/m^2; (d) $\theta_0 = 45^\circ$, $C = 298.1$ pF, $\tau = 28$ fs, $P_{ssi} = 25$ mW, $P_{osc-EPR} = 25$ mW, $\Sigma_0 = 63.6 \times 10^{-16}$ J/°C, $\Delta T = 0.11$°C, $\Delta V_{0-\mathrm{mod}} = -0.37$ mV, $\sigma_{ssi} = 17.98$ nC/m^2 and $\sigma_{osc} = 0.098$ nC/m^2.

voltage $V(t)$ is produced as described in Equation (3). In this process, $\sigma(\boldsymbol{r}, t)$ varies in time t as well as in space. The space variable $\boldsymbol{r}$ is a complex variable in the 2D space represented as $z = r_x + ir_y$, where i is the imaginary unit [1]. In the EPR the average power $P(t)$ increases exponentially until it achieves the value P_{ssi} selected for the measurement [1]. In the ssi, however, $P(t)$ sinusoidally oscillates around P_{ssi} due to the operation of the Q301 globar source affected by the temperature fluctuations of the closed sample compartment, as described in Ref. [6]. We expect the oscillations of $P(t)$ to be reflected on the

behavior of the charge density $\sigma(z,t)$.

The behavior of the average power is thus:

$$P(t) = P_{ssi} + P_{osc} \sin\left(\frac{t - t_{cP}}{H_P}\right), \tag{4}$$

where P_{osc} is the amplitude of the sinusoidal oscillations. The critical time of the power t_{cP} is the point in time in which $P(t)$ reaches P_{ssi}, while H_P is the amount of time necessary to move $P(t)$ from P_{ssi} to the crest or the trough of the sinusoidal oscillation, practically $\frac{1}{4}$ of its period [6]. According to the prediction that the surface charge density on the capacitor decreases as $\sigma(\boldsymbol{r},t) \propto \frac{1}{P(t)}$ under the illumination of the IR light, we expect that

$$\sigma(z,t) \propto \frac{1}{P(t)} \propto \frac{1}{\sin\left(\frac{t - t_{cP}}{H_P}\right)}.$$

with $z = r_x + ir_y$ and utilizing the laws of trigonometric functions for complex variables, we obtain:

$$\begin{aligned}\sigma(z,t) &\propto RE\left(\frac{1}{\sin(z,t)}\right) = RE\left(\frac{1}{\sin(r_x + ir_y,t)}\right) \\ &= \frac{1}{\sin(r_x,t)\cosh(r_y,t)} = \frac{\operatorname{sech}(r_y,t)}{\sin(r_x,t)} = \frac{\operatorname{sech}\left(\frac{v_y t - v_y t_{\sigma y}}{L_y}\right)}{\sin\left(\frac{v_x t - v_x t_{\sigma x}}{L_x}\right)}\end{aligned} \tag{5}$$

Here, v_x and v_y are the propagation velocities of the instabilities induced of the surface charge density $\sigma(\boldsymbol{r},t)$ along x and y axes, and $t_{\sigma x}$ and $t_{\sigma y}$ are the critical times for their relaxation. The quantities L_x and L_y are such that $|L_x| = |L_y| = D$, where D is the IR beam's diameter [1]. Considering σ_{ssi} and σ_{osc} the average surface charge density in the ssi and the amplitude of its deviation from equilibrium, respectively, we obtain:

$$\sigma(z,t) = \sigma_{ssi} + \sigma_{osc}\left(\frac{\operatorname{sech}\left(\frac{v_y t - v_y t_{\sigma y}}{L_y}\right)}{\sin\left(\frac{v_x t - v_x t_{\sigma x}}{L_x}\right)}\right) = \sigma_{ssi} + \sigma_{osc}\left(\frac{\operatorname{sech}\left(\frac{f_y v_y t - v_y t_{\sigma y}}{L_y}\right)}{\sin\left(\frac{f_x v_x t - v_x t_{\sigma x}}{L_x}\right)}\right) \tag{6}$$

Equation (6) suggests that the sinusoidal instability in the average power $P(t)$ produces a hyperbolic instability in $\sigma(z,t)$ modulated by a sine function. The dimensionless fractions $f_x = \frac{r_x}{L_x}$ and $f_y = \frac{r_y}{L_y}$ are defined in the next Section.

3) Determining the mechanism that transfers to the voltage $V(t)$ the fluctuations of the average power $P(t)$

While $\sigma(z,t)$ requires a spatiotemporal set of variables, the functions $\Delta V(t)$, $T_{light}(t)$, $T_{no\text{-}light}(t)$, and $\Delta T(t)$ are only time-dependent. To decouple z from $\sigma(z,t)$ and allow time t to be the only effective variable, we integrate $\sigma(z,t)$ over the area A of the capacitor illuminated by the IR light. To achieve this goal, given $z = r_x + ir_y$, in Equation (6) we write the spatial variables as follows: $r_x = f_x L_x$ and $r_y = f_y L_y$. Here, $f_x = \frac{r_x}{L_x}$ and $f_y = \frac{r_y}{L_y}$ are dimensionless fractions varying from 0 to 1 and enabling us to locate any position on the surface of area A of the capacitor [1]. For example, by choosing the origin of the reference systems on the lower left corner of a square we have that, when $r_x = 0$ and $r_y = 0$, then $f_x = 0$ and $f_y = 0$. When $r_x = D$ and $r_y = D$, then $f_x = 1$ and $f_y = 1$. With these variables, in the ssi we integrate Equation (6) over A and obtain:

$$\sigma(t) = \int_{f_{x0}}^{f_{xf}} \mathrm{d}f_x \int_{f_{y0}}^{f_{yf}} \mathrm{d}f_y \sigma_{ssi} + \sigma_{osc} \int_{f_{y0}}^{f_{yf}} \mathrm{d}f_y \operatorname{sech}\left(\frac{f_y v_y t - v_y t_{\sigma y}}{L_y}\right) \int_{f_{x0}}^{f_{xf}} \mathrm{d}f_x \csc\left(\frac{f_x v_x t - v_x t_{\sigma x}}{L_x}\right) \quad (7)$$

To solve the integrals in Equation (7) we make a substitution of the variables such that $\mathrm{X} = \frac{f_x v_x t - v_x t_{\sigma x}}{L_x}$, and $\mathrm{Z} = \frac{f_y v_y t - v_y t_{\sigma y}}{L_y}$. Thus we have $\mathrm{d}f_x = \frac{L_x}{v_x t}\mathrm{dX}$, $\mathrm{X}_0 = \frac{f_{x0} v_x t - v_x t_{\sigma x}}{L_x}$, and $\mathrm{X}_f = \frac{f_{xf} v_x t - v_x t_{\sigma x}}{L_x}$. Similarly, $\mathrm{d}f_y = \frac{L_y}{v_y t}\mathrm{dZ}$, $\mathrm{Z}_0 = \frac{f_{y0} v_y t - v_y t_{\sigma y}}{L_y}$, and $\mathrm{Z}_f = \frac{f_{yf} v_y t - v_y t_{\sigma y}}{L_y}$. With these substitutions of variables, the charge density $\sigma(t)$ becomes:

$$\begin{aligned}\sigma(t) &= \sigma_{ssi} + \sigma_{osc}\left(\frac{L_y}{v_y t}\right)\left(\frac{L_x}{v_x t}\right)\int_{\mathrm{Z}_0}^{\mathrm{Z}_f} \mathrm{dZ}\operatorname{sech}(\mathrm{Z}) \int_{\mathrm{X}_0}^{\mathrm{X}_f} \mathrm{dX}\csc(\mathrm{X}) \\ &= \sigma_{ssi} + \sigma_{osc}\left(\frac{L_y L_x}{v_y v_x t^2}\right)\left(\arctan\left(\sinh\left(\mathrm{Z}_f\right)\right) - \arctan\left(\sinh\left(\mathrm{Z}_0\right)\right)\right) \\ &\quad * \left(-\ln\left(\left|\csc\left(\mathrm{X}_f\right) + \cot\left(\mathrm{X}_f\right)\right|\right) + \ln\left(\left|\csc\left(\mathrm{X}_0\right) + \cot\left(\mathrm{X}_0\right)\right|\right)\right)\end{aligned} \quad (8)$$

For $(f_{x0}, f_{xf}) = (0,1)$ and $(f_{y0}, f_{yf}) = (0,1)$, the surface charge density $\sigma(t)$ evolves with time as:

$$\begin{aligned}\sigma(t) = \sigma_{ssi} &+ \sigma_{osc}\left(\frac{L_y L_x}{v_y v_x t^2}\right)\left(\arctan\left(\sinh\left(\frac{v_y t - v_y t_{\sigma y}}{L_y}\right)\right) - \arctan\left(\sinh\left(\frac{-v_y t_{\sigma y}}{L_y}\right)\right)\right) \\ &* \left(-\ln\left(\left|\csc\left(\frac{v_x t - v_x t_{0\sigma x}}{L_x}\right) + \cot\left(\frac{v_x t - v_x t_{\sigma x}}{L_x}\right)\right|\right)\right. \\ &\left. + \ln\left(\left|\csc\left(\frac{-v_y t_{\sigma y}}{L_y}\right) + \cot\left(\frac{-v_y t_{\sigma y}}{L_y}\right)\right|\right)\right)\end{aligned} \quad (9)$$

To know the value of $q(t)$ in the ssi requires estimating σ_{ssi}, σ_{osc}, v_x, v_y, $t_{\sigma x}$, and $t_{\sigma y}$. We assume that σ_{ssi} coincides with the values found in the

modeling of the panels shown in Figure 4. All the remaining parameters, *i.e.* σ_{osc}, v_x, v_y, $t_{\sigma x}$, and $t_{\sigma y}$, are derived from the best fit of the experimental data from Equation (1) to the model for $V(t)$ in Equation (3). The quality of the fit, shown in Figure 3, is remarkable: it highlights the effectiveness of our model for the charge density $\sigma(t)$ in the ssi based on the law of conservation of energy in Equation (2). The magnitude of $q(t)$ is of the order of fC (femto-Coulomb) [7]. In Figure 5, we used Equation (9) to picture the evolution in time of the surface charge density $\sigma(t)$ in the case corresponding to Figure 2(b), Figure 3(b) and Figure 4(b) with $\theta_0 = 0^\circ$, $C = 148.5\ \text{pF}$, $\tau = 28\ \text{fs}$, $P \cong 25\ \text{mW}$, $V_{ssi} = 3.10\ \text{mV}$, $P_{osc} = 0.25\ \text{mW}$, $\Sigma_0 = 25.9 \times 10^{-16}\ \text{J}/^\circ\text{C}$, $\Delta T = 0.27^\circ\text{C}$, $\sigma_{ssi} = 8.88\ \text{nC}/\text{m}^2$, $\sigma_{osc} = 0.00098\ \text{nC}/\text{m}^2$, $t_{cP} = 35\ \text{h}$, and $H_p = 19\ \text{h}$. In Figure 5 we clearly observe the periodic oscillations of $\sigma(t)$ mixed with non-periodic functions. The interaction between the periodic and non-periodic functions makes the evolution of $\sigma(t)$ very complex. In particular, we note an increase with time of the density of the oscillations over the capacitor area.

5. Conclusion

Capacitors respond to electromagnetic waves producing a voltage. The voltage rapidly achieves a steady state value which we derive from the law of conservation of energy. This result is important because it enables the estimation of the

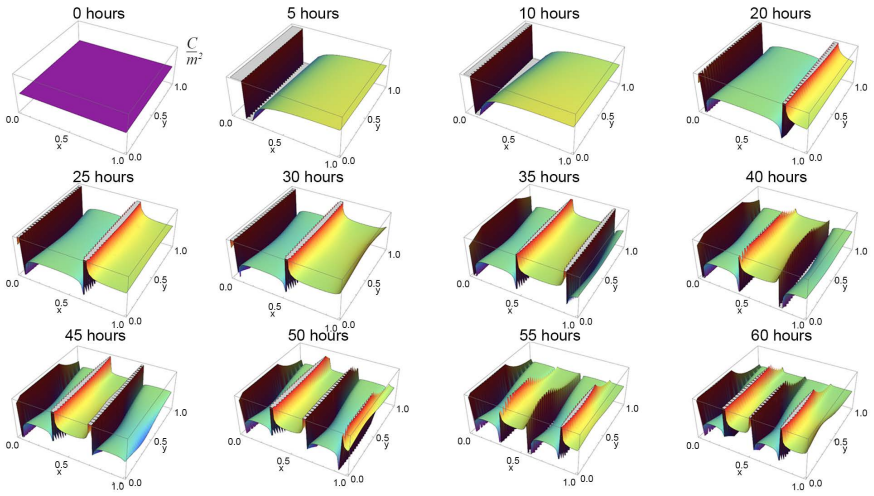

Figure 5. Here we report the surface charge densities $\sigma(t)$ evolution over the ~80 hours duration of our measurements for the case of panel (b) in Figure 2, Figure 3 and Figure 4. The parameters for this case are: $\theta_0 = 0^\circ$, $C = 148.5\ \text{pF}$, $\tau = 28\ \text{fs}$, $P \cong 25\ \text{mW}$, $V_{ssi} = 3.10\ \text{mV}$, $V_{\min} = 3.05\ \text{mV}$ occurring 60 hours after the start of the illumination, $P_{osc} = 0.25\ \text{mW}$, $\Sigma_0 = 25.9 \times 10^{-16}\ \text{J}/^\circ\text{C}$, $\Delta T = 0.27^\circ\text{C}$, $\sigma_{ssi} = 8.88\ \text{nC}/\text{m}^2$, $\sigma_{osc} = 0.00098\ \text{nC}/\text{m}^2$, $t_{cP} = 35\ \text{h}$, and $H_p = 19\ \text{h}$. The x and y axes represent the dimensionless fractions f_x and f_y, respectively. The z axis represents the surface charge density in units of nC/m^2. The surface charge density is described by Equation (9). Each panel describes the surface charge density at various instants of time (in hours).

steady state value of the voltage in other phenomena involving the interaction of electromagnetic waves with capacitors (e.g. vision in vertebrates). The result however facilitates the understanding of other phenomena in which the electromagnetic waves transfer their energy to mechanical energy or when rotational energy is transferred into the energy of the electromagnetic wave emitted in the rotation (e.g. the generation of the cosmic microwave background radiation). The relationship with the law of conservation of energy enables to track the overall effects of changes and perturbations in the various variables occurring in the phenomena. For example, we show that changes in the average power of the incident infrared light affect the surface charge density on the capacitor and thus the produced voltage.

Acknowledgements

This work was supported by the U.S. Office of Naval Research (awards # N000141410378 N000141512158), the JMU 4-VA Consortium (2016-2017), the Madison Trust—Fostering Innovation and Strategic Philanthropy—Innovation Grant 2015, the JMU Center for Materials Science, and the JMU Department of Physics and Astronomy.

Conflicts of Interest

The authors declare no conflicts of interest regarding the publication of this paper.

References

[1] Boone, D.E., Jackson, C.H., Swecker, A.T., Hergenrather, J.S., Wenger, K.S., Kokhan, O., Terzić, B., Melnikov, I., Ivanov, I.N., Stevens, E.C. and Scarel, G. (2018) Probing the Wave Nature of Light-Matter Interaction. *World Journal of Condensed Matter Physics*, **8**, 62-88. https://doi.org/10.4236/wjcmp.2018.82005

[2] Sarker, B.K., Cazalas, E., Chung, T.-F., Childres, I., Jovanovic, I. and Chen, Y.P. (2017) Position-Dependent and Millimeter-Range Photodetection in Phototransistors with Micrometer-Scale Graphene on SiC. *Nature Nanotechnology*, **12**, 668-674. https://doi.org/10.1038/nnano.2017.46

[3] University of Colorado at Boulder. The Average Solar Irradiance Is 136.05 mW/cm^2 according to Data Provided by the Laboratory for Atmospheric and Space Physics.

[4] Soum-Glaude, A., Le Gal, A., Bichotte, M., Escape, C. and Dubost, L. (2017) Optical Characterization of $TiAlN_x/TiAlN_y/Al_2O_3$ Tandem Solar Selective Absorber Coatings. *Solar Energy Materials & Solar Cells*, **170**, 254-262. https://doi.org/10.1016/j.solmat.2017.06.007

[5] Gawiser, E. and Silk, J. (2000) The Cosmic Microwave Background Radiation. *Physics Reports*, **333-334**, 245-247. https://doi.org/10.1016/S0370-1573(00)00025-9

[6] Gordon, A.L., Schwab, Y., Lang, B.N., Gearhart, G.P., Jobin, T.R., Kaczmar, J.M., Marinelli, Z.J., Mann, H.S., Utter, B.C. and Scarel, G. (2015) Decoupling the Electrical and Entropic Contributions to Energy Transfer from Infrared Radiation to a Power Generator. *World Journal of Condensed Matter Physics*, **5**, 301-318. https://doi.org/10.4236/wjcmp.2015.54031

[7] St. John, T.C., Marinelli, Z.J., Kaczmar, J.M., Given, R.P., Wenger, K.S., Utter, B.C. and Scarel, G. (2016) Conversion of Infrared Light into Usable Energy. *Proceedings of SPIE*, **9927**, 99270C.

[8] Vermeulen, L.A. and Wintle, H.J. (1970) Infrared Photoelectric Effects in Polyethylene. *Journal of Polymer Science Part A*-2: *Polymer Physics*, **8**, 2187-2195. https://doi.org/10.1002/pol.1970.160081214